

## Thermodynamic Simulation as an Assistant Tool in the Development of Iron Based Hardfacing Materials

Edmilson Otoni Correa<sup>a\*</sup>, Nelson Guedes de Alcântara<sup>b</sup>,

Dorival Gonçalves Tecco<sup>c</sup>, Ramachandan Vasant Kumar<sup>d</sup>

<sup>a</sup>Universidade Federal de Itajubá – UNIFEI, Av. BPS, 1303,  
Pinheirinho, 37500-903 Itajubá - MG, Brazil

<sup>b</sup>Universidade Federal de São Carlos – UFSCar, Departamento de Materiais,  
Rod. Washington Luis, CP 676, 13565-905 São Carlos - SP, Brazil

<sup>c</sup>Welding Alloys Ltd, The way, Fowlmere, Royston, Herts, United Kingdom

<sup>d</sup>Department of Materials Science and Metallurgy, University of Cambridge,  
Pembroke Street, Cambridge, United Kingdom

Received: March 26, 2007; Revised: August 8, 2007

A thermodynamic model was used to investigate the solidification of a hardfacing material in Fe-Cr-C-Nb system designated CNO, and developed for cladding components subjected to severe abrasive wear by welding. Microstructural characterization of the alloy showed that the theoretical simulations carried out to predict the amount and volume fraction of the phases using the module Scheil of MT-DATA Software gave very realistic results in the case of the rapid solidification of the hardfacing alloy CNO. The results obtained in this study indicate that the utilization of this tool may provide a good understanding of alloys solidification. As a consequence, it is possible to enable the refinement of alloy composition during the early stages of hardfacing materials development, leading to a decreasing of overall cost and time of manufacturing of hardfacing electrodes.

**Keywords:** *development, hardfacing materials, thermodynamics simulations*

### 1. Introduction

It is well established that variations in the alloy content have a significant effect upon the nature and volume fraction of carbides and retained austenite during the solidification of iron based hardfacing materials. These microstructural differences, in turn, have an important effect upon weld metal cracking susceptibility and wear properties<sup>1</sup>. However, to predict these effects upon wear properties and enable the optimization of alloy composition is one of the problems to consider during any hardfacing alloy development.

A useful experimental technique used to investigate the solidification of the alloys, consist of the utilization of thermal analysis and solidification interruption by specimen freeze. In this technique, the specimen is inserted into a ZAS crucible, which are fed into a resistance furnace and heated in a inert argon atmosphere. As soon as the specimen reaches a specified temperature, it is immediately cooled in a ice/water bath. Then, its microstructure is observed to identify the phases present in that temperature. This procedure is repeated for several temperatures from the fusion temperature of the specimen in order to obtain its solidification curve. More details of this technique can be found elsewhere<sup>2</sup>.

However, as the application of this technique requires furnace, thermocouples, crucibles, etc., the solidification study usually is longer and more expensive. Furthermore, the results may be not precise enough because the solidification process is prone to occur rapidly and continuously and in this technique the solidification is considered to occur in several temperature stages.

Due to these problems in utilizing experimental techniques, thermodynamics simulations have been often used to theoretical study of solidification of several new alloy systems, mainly under thermodynamic equilibrium conditions (ex. sand casting process).

However, little has been published regarding the non-equilibrium solidification conditions usually present in welding process. This paper therefore describes the utilization of thermodynamic simulations to provide the basis for understanding the alloy solidification mechanisms and thus enable the optimization of alloy composition (for instance by reducing the amount of intermetallic phases which decrease the wear resistance). A realistic alloy solidification model can be obtained using thermodynamic and kinetic data, provided that the model is validated experimentally. In the case of hardfacing materials, given that at relatively high energy input, weld metal usually experiences high cooling rates, the microstructure obtained in weld deposits is far from equilibrium. Thus, the fact that non-equilibrium solidification occurs was taken into account in the solidification model, which led to the choice of the Scheil simulation module of MT-DATA, in conjunction with the *plus* and *sub-sgte* databases<sup>3</sup>. In a Scheil simulation, calculations rely on the assumption that no diffusion occurs in the solid, and that perfect mixing occurs in the liquid owing to efficient stirring, which is adequate for the rapid cooling of weld metal<sup>4</sup>.

MT-DATA, in turn, comprises of an integrated suite of software to calculate chemical and physical equilibria using thermodynamics data for systems of industrial importance. It predicts equilibrium phases in systems containing many elements and many phases, based upon critically assessed thermodynamic data for simpler sub-systems using a Gibbs energy minimization algorithm. The output is only as good as the input and MT-DATA results must be used by informed researchers only. The user has to input the system elements (eg. Fe, Cr, C, Mn, etc) amounts, temperature, pressure/volume and, the MTDATA software rapidly and automatically refers to the available databases

\*e-mail: ecotoni@unifei.edu.br

to obtain thermodynamic data for these species. The output of the MTDATA calculations is either in tabular columns or in diagrams of the form of binary/ternary diagrams, predominance area diagrams, isopleths, liquidus projection, etc.<sup>3</sup>.

## 2. Experimental work

### 2.1. Fabrication of hardfacing consumables

A versatile processing route was used for the manufacture of hardfacing cored consumable. In this case, a steel shaped sheath was filled with the mixing of various commercial powders, as illustrated in Figure 1. The wire was then conformed down to a diameter of 2.8 mm by rolling and spooled. The nature and amount of powders inserted in the sheath per unit length were determined with a help of a computer program.

Hardfacing was done on a mild steel plate using the conditions shown in the Table 1. The weld deposit consisted of four layers overlapped and was processed by depositing several beads using the open arc welding process. This procedure enabled to eliminate the effect of the dilution upon the microstructure of the hardfaced layer.

The chemical composition of the undiluted top layer of the alloy, obtained by optical emission spectrometry, is shown in Table 2. The alloy designated CNO is a high-chromium white iron with addition of Nb.

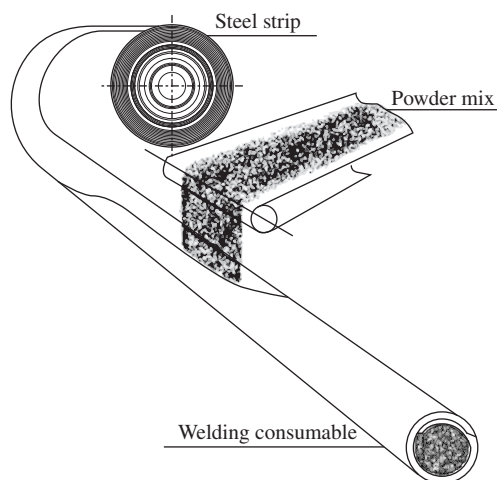


Figure 1. Principle of cored welding wire manufacture.

Table 1. Welding conditions.

Arc voltage	28 a 31 V (DC)
Welding current	450 a 500 A
Electrode polarity	Positive
Wire feeding rate	4.5 m/min
Traveling speed	1.5 m/min
Preheating	N°
Electrode angle	10° to plate surface
Stick-out	30 mm
Bead step over	6 mm
Bead type	Stringer (no oscillation)
Deposition rate	≈7.5 kg.h <sup>-1</sup>

### 2.2. Microstructural characterization

The hardfaced specimens were sectioned transversal to the surface then polished and etched with Villela reagent. Microstructural examination of the specimens was carried out using standard optical microscopy and scanning electron microscopy (SEM). Energy dispersive spectrometry (EDS) facilities available on an SEM enabled analysis of individual phases present in the alloy and their chemical compositions to be obtained. Procedures involving heavy etching of specimens were also used to perform quantitative analyses of phases. Image processing and an image analysis computer program were subsequently used to determine the volume fraction of phases.

## 3. Results and Discussion

### 3.1. Theoretical solidification study

The solidification sequence of CNO calculated assuming non-equilibrium conditions is shown in Figure 2. Niobium carbide is the first solid phase to become thermodynamically stable, which precipitates from the liquid at ~1971 °C. The weight fraction of NbC then gradually increases over a wide range of temperatures until the alloy reaches 1347 °C. Solidification then proceeds with the massive precipitation of  $M_7C_3$  between 1347 and 1235 °C. The formation of austenite begins at about 1235 °C as 65% of liquid still remains and no more NbC is expected to form below that temperature.  $M_3C$  is expected to form between 1135 and 935 °C together with some  $M_7C_3$  and additional austenite.

Studying the nature of phases forming close to the alloy eutectic temperature was of little interest, as the volume fraction of these phases clearly is negligible and requires thorough examination (for

Table 2. Chemical composition (wt. (%)) of top layer of the alloy CNO, in as-welded condition (four layer deposits).

Hardfacing electrode	C	Si	Mn	Cr	Ni	Nb	Ti	V
CNO	4.8	0.9	0.7	21.6	-	6.5	-	-

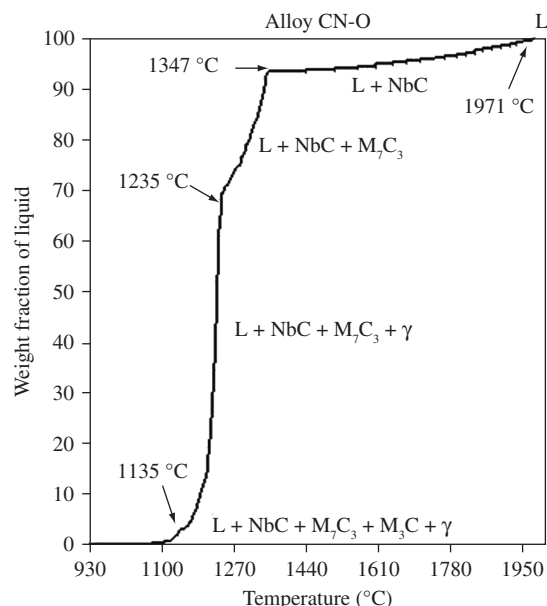
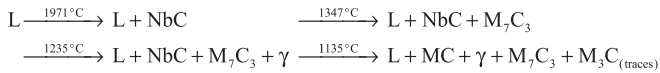


Figure 2. MTDATA/Sheil simulation showing weight fraction of liquid present in CNO as function of temperature.

instance by X ray diffraction) to validate their occurrence. MT-DATA was also useful to calculate the theoretical volume fraction of stable thermodynamically phases in the alloy CNO during the solidification (see Figure 3). From this figure, as can be seen that after complete solidification, just over 53 wt. (%) of austenite phase is present with the remaining 47 wt. (%) being divided between the carbides ( $\text{NbC} - 7 \text{ wt. } (\%)$ ;  $\text{M}_7\text{C}_3 - 39 \text{ wt. } (\%)$ ;  $\text{M}_3\text{C} - 1 \text{ wt. } (\%)$ ).

On the basis of the results of the simulation, the solidification of CNO can be summarized as follows:



### 3.2. Microstructural characterization

Microstructural examination of polished surface of undiluted top layer of hardfaced alloy CNO under optical microscope revealed the presence of randomly dispersed phase, labeled A in Figure 4.

After etching, the most striking feature of CNO is the presence of a high volume of bright large particles. Depending on where the observation is carried out in the specimen, these particles appear mostly as needles (which can reach over 0.5 mm in length), but also as hexagonal particles, as can be seen in Figure 5.

Phase A (gray particles) can be distinguished at high magnification (Figure 6) and it is important to note that the matrix (M) of CNO is composed of two main phases, one of which is etched, while other remains resistant to chemical attack. It is worthwhile noting again the random distribution of phase A: individual particles are often surrounded by the matrix, but can also be found alongside or inside phase B, which appears to grow around phase A. Work carried out by previous investigators on an iron-base hardfacing alloy with similar composition, showed the presence of  $\text{NbC}$  and  $\text{M}_7\text{C}_3$  - type carbides, the morphology of which is that the phases A and B, respectively<sup>5,6</sup>. The needle-shape morphology of phase B is a typical feature of Cr-rich  $\text{M}_7\text{C}_3$  found in hypereutectic high chromium deposits<sup>6</sup>. Early

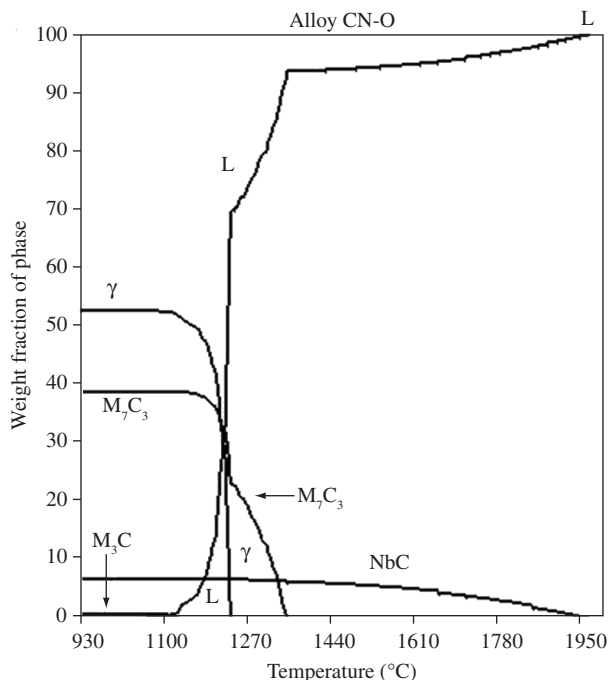


**Figure 3.** Calculated equilibrium weight fraction of phases in CNO as a function of temperature.

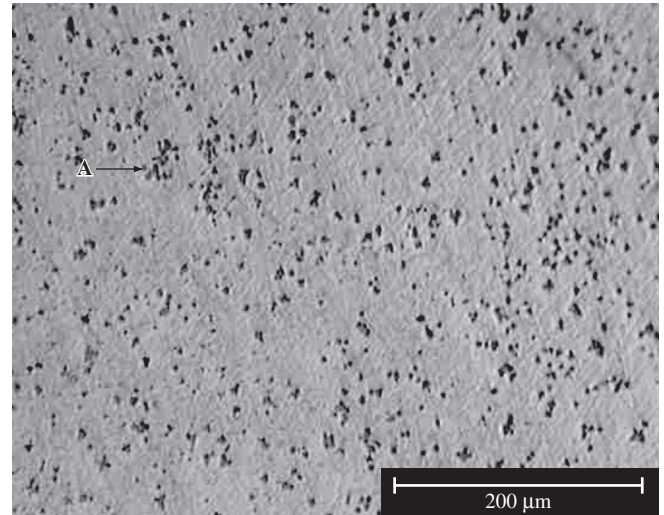


**Figure 4.** Micrograph of the polished surface of CNO showing the presence of randomly dispersed particles (phase A).

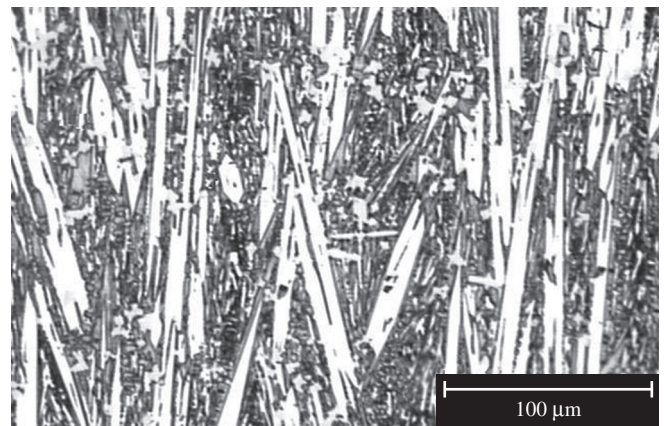


**Figure 5.** Microstructure of CNO roughly along the heat flow direction, showing an array of coarse bright needle-shape and some hexagonal particles.

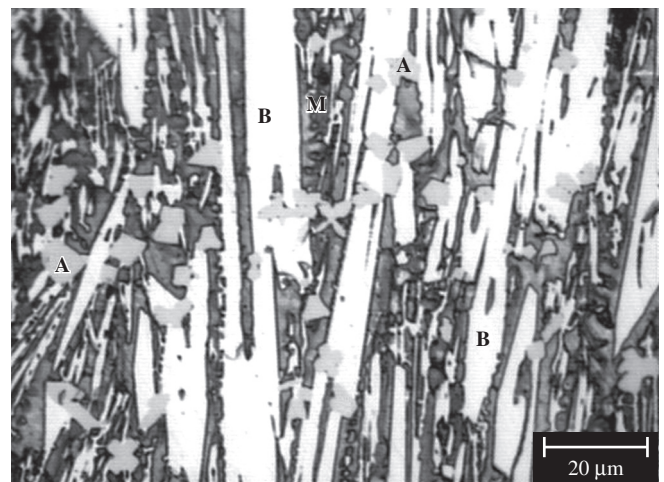


**Figure 6.** Labeling of main phases present in CNO: A randomly dispersed phase; B needle-shape/hexagonal particles; M matrix with parts resistant to chemical attack and dark gray etched parts.



work has shown that  $M_7C_3$  needles grow predominantly along the heat flow direction in layer deposits<sup>7</sup>.

Microstructural observation of a CNO specimen in the as welded condition in back-scattered imaging mode in the SEM revealed that

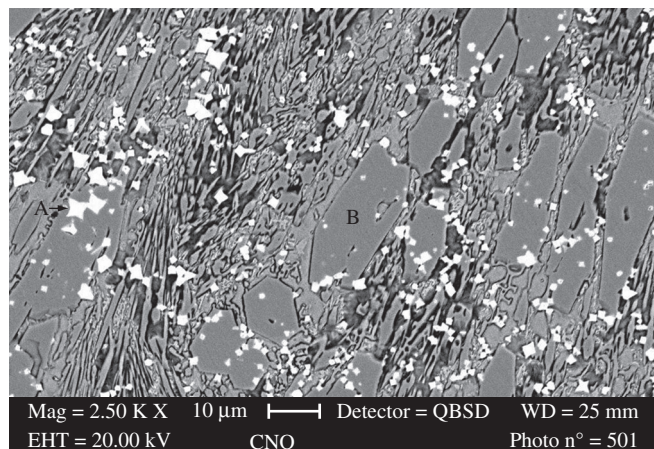


**Figure 7.** Back scattered electron image of CNO showing good contrast between phases. A-fines NbC carbides, B-  $M_7C_3$  carbides and M-Matrix comprised of eutectic mixture  $\gamma/M_7C_3$ .

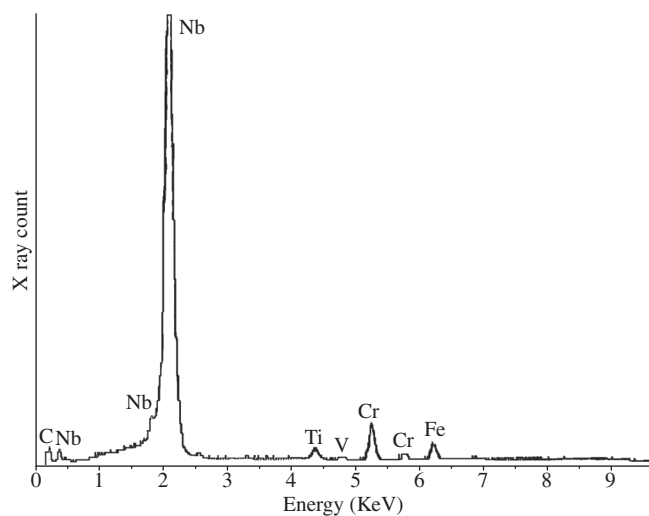


**Figure 8.** Semi-quantitative chemical analysis of phase A using SEM. Nb is the prime constituent.

**Table 3.** Typical chemical composition obtained for main phases present in CNO by EDS analysis, ignoring carbon content (wt. (%)).

Phase	A	B	M (region 1)	M (region 2)
Si	-	-	1.20	0.87
Nb	78.77	0.49	0.51	1.10
V	0.05	-	-	-
Cr	10.85	60.01	28.31	53.60
Mn	-	-	2.26	-
Fe	6.43	38.34	67.72	44.43
Ti	2.67	-	-	-
Ni	-	-	0.22	-

phase A is enriched with one element with high atomic number (cf. Figure 7), which was confirmed by EDS (Figure 8 and Table 3). Phase A was found to be largely enriched in Nb. Traces of Cr, Ti, V and Fe were also found in addition to the presence of C.

Although EDS system used did not enable a reliable quantitative measurement of carbon to be obtained, results obtained so far together with information found in the literature strongly suggest that phase A is NbC carbide. EDS data shown in Figure 9 and Table 3 indicates that phase B is a carbide enriched with Cr and Fe, which further supports the hypothesis that this phase is primary  $M_7C_3$ . Chemical microanalysis in two different regions of the matrix M showed that this region was widely enriched of Cr and Fe (Figure 10a, 10b and Table 3). These results and the morphology of the phases strongly indicate that region M is eutectic mixture  $\gamma$  (austenite)/ $M_7C_3$ <sup>8</sup>.

Results obtained from image analysis in order to estimate the volume fraction of the phases present in alloy CNO are shown in Table 4. The slightly etched polished surfaces of metallographic specimens were used to obtain good contrast of the fine phase. Heavy etching completely removed the matrix (phase M), which only left phase B apparent. On the basis of the relationship between area and volume fractions, results show that the average volume fraction of phases A is approximately 6.8%. As the matrix has been completely removed by deep etching, image analyses results also show that phase B roughly compose 40% of the hardfacing.

Therefore, as can be seen from the microstructural characterization results obtained, the main phases predicted in the solidification of the alloy CNO (see Figure 1) was precisely identified. It can be seen also that the results shown in Table 4 for each main phase presented a good concordance with the results obtained by the theoretical

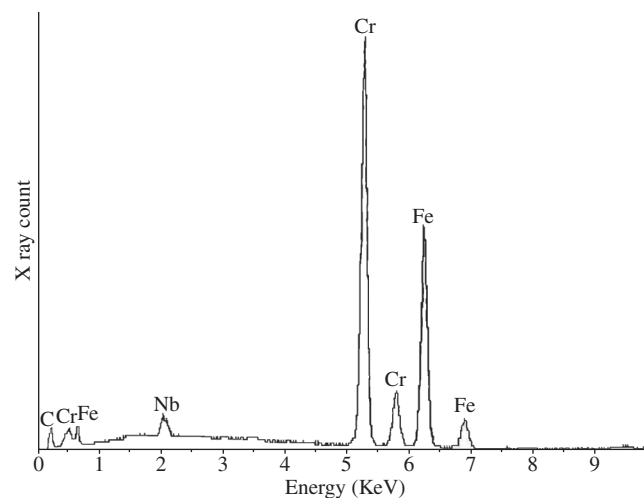


**Figure 9.** Semi-quantitative chemical analysis of the phase B using SEM. Cr and Fe is the prime constituents.

**Table 4.** Image analysis results.

Alloy CNO			
Statistical function	Phase A (NbC)	Phase B ( $M_7C_3$ )	Phase $\gamma$ (Austenite)
Unity	%	%	%
Counts	15	15	15
Mean	6.77	39.66	53.57
Standard deviation	0.89	2.82	2.82

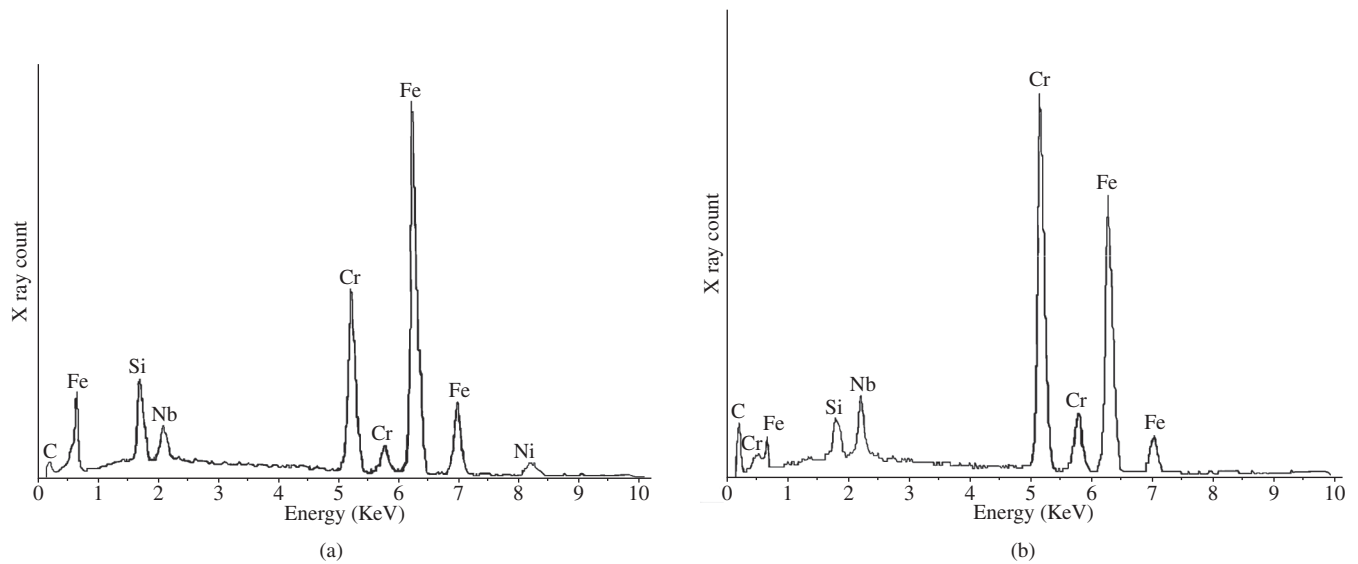


**Figure 10.** Semi-quantitative chemical analysis of phase M. a) in region 1 using SEM. Fe and Cr is the prime constituents; and b) region 2 using SEM. Cr and Fe is the prime constituents.

simulation of volume fraction in Figure 2. Thus, the application of Scheil solidification module of the MTDATA software enabled the obtaining of very realistic results of solidification of the hardfacing material CNO.

#### 4. Conclusions

The present paper showed that the application of thermodynamic simulations, using the module Scheil of MT-DATA software, to predict the non-equilibrium solidification of hardfacing alloys gave very realistic results. Therefore, these thermodynamic simulations may be a useful and cost effective tool to be used during any development of new abrasive wear resistant hardfacing materials.

#### Acknowledgments

The authors are grateful to Welding Alloys Ltd (UK) for providing welding consumables and equipments. The authors also thank Prof. H.K.D.H Bhadeshia for the provision of MT-DATA software and the Brazilian Organization, CNPq.

#### References

1. Scandella F, Scandella R. Development of hardfacing materials in Fe-Cr-Nb-C system for use under highly abrasive conditions. *Materials Science and Technology*. 2004; 20(1):93-105.
2. Gregolin JAR. *Desenvolvimento de ligas Fe-C-Cr-Nb resistentes ao desgaste*. [D. Phil. thesis]. Campinas: Universidade de Campinas; 1990.
3. MTDATA 4.70. *User's Guide*. Teddington: National Physical Laboratory; 2004.
4. Porter DA, Easterling KE. *Phase transformations in metals and alloys*. second ed. London: Chapman and Hall; 1994.
5. Atamert S, Bhadeshia HKDH. Microstructure and stability of Fe-Cr-C hardfacing alloys. *Materials Science and Engineering*. 1990; 130(2):101-111.
6. Atamert S. Stability, wear resistance and microstructure of iron, cobalt and nickel-based hardfacing alloys. [D. Phil. Thesis]. Cambridge: University of Cambridge. 1988. p. 149-177.
7. Avery HS, Chapin, HJ. Hardfacing alloys of the chromium-carbide type. *Welding Journal*. 1952; 49(3):175-182.
8. Metals Handbook. *Metallography and phase diagrams*. (4). ninth ed. Ohio: ASM International; 1983.

